



# Thermistor string corrections in data from very weakly stratified deep-ocean waters<sup>☆</sup>

Hans van Haren

NIOZ Royal Netherlands Institute for Sea Research, P.O. Box 59, 1790, AB Den Burg, the Netherlands

## ARTICLE INFO

### Keywords:

High-resolution temperature measurements  
Long-term deep-ocean moorings  
Drift corrections  
Comparison with CTD-Stability

## ABSTRACT

An important parameter for observational studies on dynamical variations of the ocean is temperature (T) which determines density variations together with salinity. While the achievement of high absolute accuracy of T-sensors is a formidable task, even the maintaining of high precision is difficult for any long-term deep-ocean observations. This is because the deep ocean is very weakly stably stratified in density, in which all the dynamics is covered by a range of about 0.001 °C. One requires high-resolution T-sensors with low noise levels and precisely calibrated. However, common Negative Temperature Coefficient (NTC) thermistor T-sensors have electronic drift causing a bias of temperature with time. The drift rate varies with temperature (change) and time (age) between 0.0002 and 0.001 °C wk<sup>-1</sup> for T-sensors used here. A string of such T-sensors moored in the open-ocean for more than a month after calibration requires a drift-correction. When moored in the deep-ocean, a secondary correction is necessary even immediately after calibration. Secondary correction uses reference layers that are homogeneous to within 0.00005 °C over 100 m vertically plus an additional polynomial correction to remove remaining bias prior or after the reference date. Secondary correction may also involve pressure information on surface tides and mooring deflection. In this paper, secondary corrections are described for two cases of data. For one case from the West-Mediterranean varying temperature-density relationship and near-homogeneous conditions exist. The other is from hadal-deep instruments on a long mooring line in the Challenger Deep, Mariana Trench, affected by tidal flow. Nearby shipborne CTD-data are always needed to establish the temperature-density relationship and the background vertical temperature slope to which the moored T-sensor data are referenced. The stability of moored T-sensors is compared with that of temperature sensors of CTD.

## 1. Introduction

One of the difficulties in studying dynamical processes in the deep-sea is the remoteness. One needs a ship to lower scientific instrumentation. The instrumentation has to withstand high static ambient pressure to protect its modern-day electronics from salt-water destruction. Another difficulty is the small variation in values of observable parameters which requires high-precision and delicate instrumentation. Because of the small variations in values of environmental variables, the instrumentation requires high stability, also for modern-day electronics, to minimize artificial data such as due to instrumental drift.

The here presented corrections for bias of Negative Temperature Coefficient (NTC) thermistors (thermal resistors of semiconducting material observed in 1833 by M. Faraday, <https://www.computerhistory.org/siliconengine/first-semiconductor-effect-is-recorded/>) may be of

interest for internal wave and turbulence studies and for deep water mass analysis observations. Deep-sea internal wave dynamics are governed by temperature variations of typically  $\pm 0.001$  °C. Water masses are characterized by certain ranges of parameter characteristics like temperature and salinity, and in the deep-ocean these ranges are relatively narrow and well-defined. For example, Antarctic Deep Water (AABW) is defined near its source by  $34.830 \pm 0.009$  g kg<sup>-1</sup> in Absolute Salinity and  $-0.46 \pm 0.24$  °C in Conservative Temperature (e.g., [Liu and Tanhua, 2021](#)). In the vicinity of the equator AABW is defined by other characteristics (e.g., [Rhein et al., 1998](#)). The above AABW-ranges reflect variations in deep dense water mass formation, from month to month, year to year and decade to decade, variations due to turbulent mixing with adjacent waters, and, possibly, instrumental errors such as bias of not recently calibrated instrumentation. Given the above ranges, the instrumental bias for one-year old calibrations of shipborne SeaBird 911

<sup>☆</sup> Hans van Haren reports financial support was provided by NWO, the Netherlands Organization for the advancement of science.

E-mail address: [hans.van.haren@nioz.nl](mailto:hans.van.haren@nioz.nl).

<https://doi.org/10.1016/j.dsr.2022.103870>

Received 15 December 2021; Received in revised form 22 August 2022; Accepted 26 August 2022

Available online 31 August 2022

0967-0637/© 2022 The Author. Published by Elsevier Ltd. This is an open access article under the CC BY license (<http://creativecommons.org/licenses/by/4.0/>).

Conductivity Temperature Depth (CTD) instruments is only a small fraction of the temperature range, bias of  $0.0025\text{ }^{\circ}\text{C y}^{-1}$ , but a non-negligible part of the salinity range, bias of  $0.003\text{ g kg}^{-1}\text{ y}^{-1}$  (SeaBird, 2015, 2016, Sections 2, 3).

In less open deep basins, such as in trenches or semi-enclosed seas, deep water masses may vary less due to natural processes and temperature bias may not be negligible in comparison with the local water mass range definition. Such knowledge may be important for studies on the spreading and aging of deep dense waters. As will be discussed, deep-sea dynamics on, e.g., internal waves and turbulent exchange and transport, require relative temperature precision to within  $0.0001\text{ }^{\circ}\text{C}$ . Such precision needs to be achieved under very different conditions from those of a laboratory and is potentially more feasible for instruments on a well-designed taut-wire mooring than lowered on a cable from a ship riding surface waves. It is questionable whether absolute accuracies to within less than  $0.0001\text{ }^{\circ}\text{C}$  would be achievable in deep-ocean moored instrumentation, because well-calibrated reference instrumentation barely exists and, if existent, cannot be easily compared with the deep moored instrumentation.

Like piezo crystals and various other electronic measurement devices, a temperature (T-)sensor consisting of NTC-thermistors placed in a Wien bridge is known to show drift or bias (stability variations) of temperature with time. The drift is considered a slowly varying non-linear function (e.g., Wood et al., 1978; Kulkarni et al., 2015). Its rate depends on temperature and on time, but generally to unknown extent. Aging of sensors changes the drift characteristics, with generally lower rates for older than for newly built sensors. For example, the NTC-thermistors combined with the connected electronics in moorable self-contained high-resolution T-sensors typically drift at a rate of  $0.001\text{ }^{\circ}\text{C wk}^{-1}$ , which changes to less than  $0.001\text{ }^{\circ}\text{C mo}^{-1}$  over time after aging and/or after deployment longer than a month in a new ocean environment with different ambient temperature (Cimatoribus et al., 2016) and, possibly, different pressure.

Drift usually artificially increases temperature with time, but some sensors show decreasing drift temperature. Subtle differences exist between individual sensors. No general drift correction can be applied to within a certain error. During the post-processing of T-sensor data from a laboratory isothermal bath, the non-linear drift can be corrected to within approximately  $0.0001\text{ }^{\circ}\text{C}$  as measured from the well-calibrated reference thermometer (Cimatoribus et al., 2016). Under laboratory conditions T-sensors can also be calibrated every day if necessary, albeit to within certain range and capacity limitations.

In a mooring in the deep-ocean however, a daily calibration is impossible and a reference thermometer does not exist. Therefore, for the case of a string of moored T-sensors, the vertical temperature slope from one-day averaged values may be compared with nearby shipborne profiling high-resolution CTD measurements. This method works well under moderate-to-strongly stratified ocean conditions in which the buoyancy frequency  $N > 10f$ ,  $f$  denoting the inertial frequency, so that the buoyancy period is considerably smaller than one day. Drift inferred from two different calibrations prior to mooring deployment and after recovery is insufficient for correction because the drift's non-linearity and temperature- and time-dependence are not accounted for. Remaining drift will be  $O(0.001\text{ }^{\circ}\text{C})$  after linear correction, for a drift  $O(0.01\text{ }^{\circ}\text{C})$  without correction.

As will be demonstrated in this paper, in near-homogeneous waters where  $N = O(f)$  the vertical pressure-compensated temperature slope amounts  $d\theta/dz \approx 0.0005\text{ }^{\circ}\text{C}/100\text{ m}$  and small-scale dynamical temperature variations are measured to be  $< 0.0001\text{ }^{\circ}\text{C}$ . In such waters, drift-correction of moored T-sensors require a different approach. The large-scale vertical temperature slope from CTD-data can still be used as reference even when varying over time, but a secondary correction is required. In this paper, specific corrections will be discussed for moored T-sensor data from two different deep-sea sites.

Instrumental details are described in Section 2. CTD-data and their stability in comparison with moored T-sensors are discussed in Section

3. Results of corrections are provided for studying phenomena like seafloor convection using a relatively short taut-wire T-sensor mooring in deep near-homogeneous West-Mediterranean waters with variable temperature-density relationship and negligible tidal flow in Section 4, and turbulent overturning using a more deflecting very long mooring in weakly stratified waters with tidal flows in the deep Mariana Trench in Section 5. Some general findings also for other temperature sensors are discussed together with a resume of conclusions in Section 6.

## 2. Instrumental details

### 2.1. Moored T-sensors

'Nederlands Instituut voor Onderzoek der Zee' NIOZ4 are independent, self-contained T-sensors with single sample data having a precision better than  $0.0005\text{ }^{\circ}\text{C}$  and a noise level of less than  $0.0001\text{ }^{\circ}\text{C}$  (van Haren, 2018). They are constructed to be moored in a vertical string of typically 100 sensors and can be left unattended for a year whilst sampling at a rate of about 1 Hz. The vertical coordinate  $z(\text{m})$  of the Cartesian  $[x, y, z]$  system equals zero at the ocean-surface and measures positive values in the atmosphere and negative values in the ocean. Bad or missing data records, e.g. due to battery problems or other electronic and mechanic failure, are linearly interpolated between those of neighbouring sensors. T-sensors are taped at typically 1–2 m intervals to  $0.0063\text{ m}$  diameter nylon-coated steel cables. Every 4 h, the internal clocks of all sensors on a mooring are synchronized via induction through the steel cable to a single standard clock, so that sampling times are less than  $0.02\text{ s}$  off. Thus, almost instantaneously a near-vertical temperature profile is obtained over a range  $O(100)\text{ m}$ , when the mooring-line is kept taut by sufficient sub-surface buoyancy. These T-sensors have been designed for studies on internal waves and turbulent overturning in the ocean, for which high precision is required but absolute accuracy is of less importance.

After application of laboratory-bath calibration, moored T-sensor data are corrected for slight compressibility effects by transfer to Conservative Temperature  $\Theta$  using the Gibbs-Sea-Water-software described in (IOC et al., 2010). Although  $\Theta$  will be used throughout, they will mainly be described as 'temperature' for short henceforth.

As outlined by (van Haren et al., 2013; Cimatoribus et al., 2016) a common method to correct for drift in moored T-sensor data obtained from well-stratified waters is to establish a mean vertical temperature slope that is referenced to such a slope from nearby CTD-data. The averaging period for the moored data should certainly be longer than the buoyancy period, to remove turbulence, and preferably longer than the inertial period, to remove turbulence also in weakly stratified layers. A preferred typical averaging period is 4–7 days long. Ocean-data averaged over a few days do not contain any turbulent overturning and thus reflect stably stratified waters by nature. Averaging over a period longer than 7 days risks the inclusion of drift ( $\geq 0.0002\text{ }^{\circ}\text{C}$ ) that may spoil natural observations. To the drifted data a smooth, but de facto necessarily vertically stable temperature profile can be fitted using a polynomial function, typically of order 2. This common drift-correction by replacing the drift-affected mean data by the polynomial function is applied to all moored T-sensor data presented in this paper together with the above calibration and pressure-(compressibility) correction.

Subsequent special corrections are presented and applied here for two different cases in weakly stratified waters in the deep-sea. For such corrections also nearby shipborne CTD-data are required, which should have high accuracy.

### 2.2. CTD-accuracy

In order to put the drift or stability of  $0.001\text{ }^{\circ}\text{C mo}^{-1}$  of NIOZ4 T-sensors in perspective, it is theoretically verified against that of standard high-accuracy oceanographic SBE CTD-equipment. SeaBird SBE user manuals of both SBE911 (SeaBird, 2015) and SBE19 (SeaBird, 2016)

CTDs, and their brochures of 2021, show that the stability of the sensors is non-negligible. It is  $0.0002\text{ }^{\circ}\text{C mo}^{-1}$  for temperature and  $0.0003\text{ S m}^{-1}\text{ mo}^{-1}$  for conductivity. The temperature stability is in line with a few  $0.001\text{ }^{\circ}\text{C y}^{-1}$  found in typical laboratory test sensors by Kulkarni et al. (2015). Although SeaBird's technical manuals indicate that the above stability values indicate an error, they do not explicitly state what that means: A random error increase, or a bias. A bias is common, and often called drift, for resistors as in T-sensors (Wood et al., 1978). Here, we treat them as drift.

The quoted stability value for SBE temperature sensors is small, five times smaller than that for aged NIOZ4 T-sensors, but may be plausible. The reported stability value for SBE conductivity sensors (SeaBird, 2015, 2016) is unrealistic as it would imply a large drift of  $0.0025\text{ g kg}^{-1}\text{ mo}^{-1}$  in salinity, for deep Mediterranean waters. To be comparable to the drift

in the SBE temperature sensors it is hypothesized that the conductivity/salinity drift should be at least a factor of 10 smaller. It is suggested a mistake in the conductivity units in the SBE manual ( $\text{mS cm}^{-1}$  should be  $\text{S m}^{-1}$ ) leads to this unrealistic drift.

CTD-observations cannot be improved in their accuracy by comparing their data with in-situ sampled reference data. Except perhaps when using a recently calibrated SeaBird SBE35 Deep Ocean Standards Thermometer, used rarely in the ocean, next to the SBE3, water sampling does not improve the absolute accuracy of SBE911 temperature data over a one-year old or more recent calibration of its sensors. The most precise laboratory measurement against a seawater standard is no more accurate than  $0.002\text{ g kg}^{-1}$  using a Guildline 8400B Autosol.

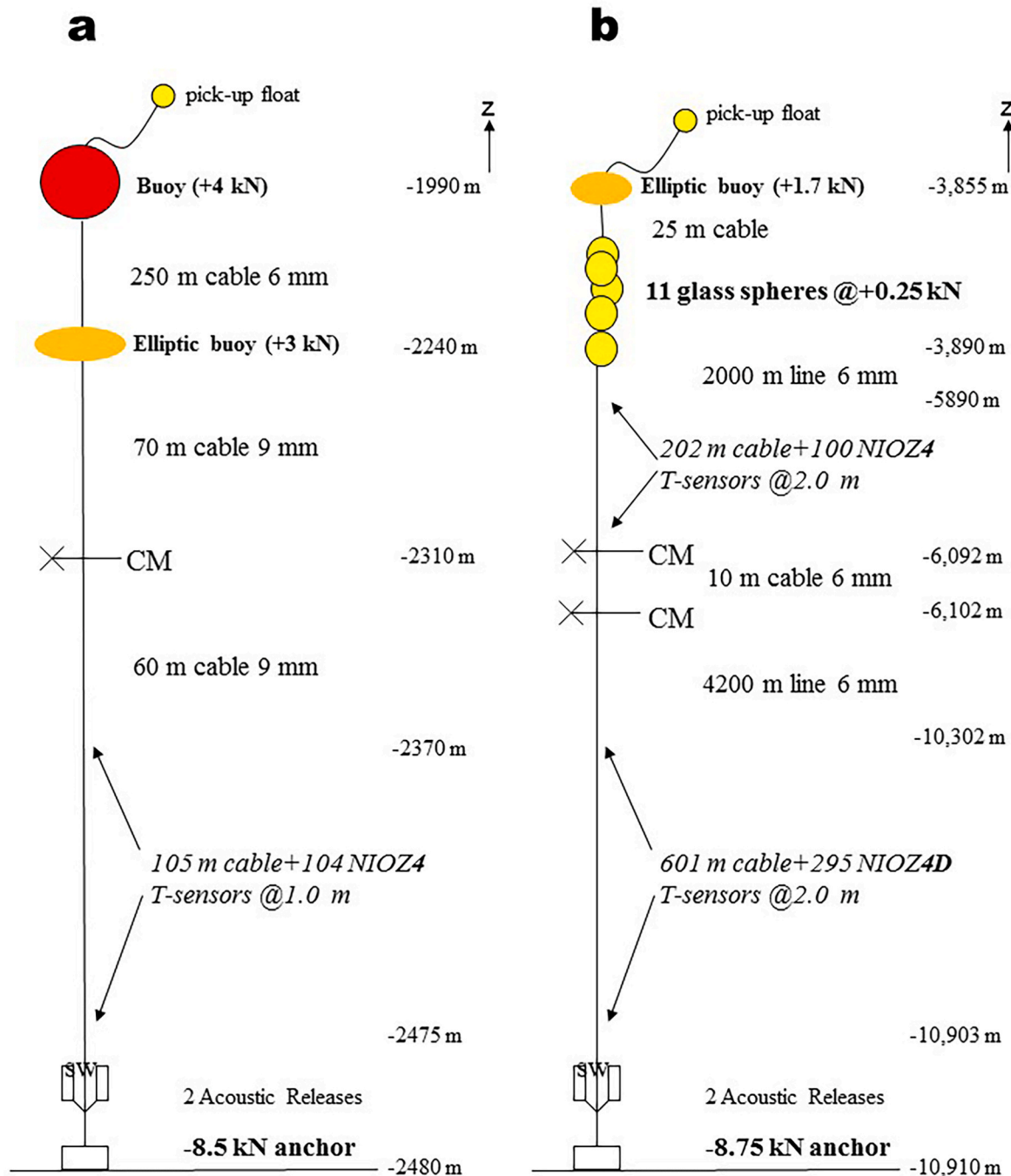


Fig. 1. Mooring diagrams (not to scale). (a) West-Mediterranean Sea mooring. (b) Challenger Deep mooring.

### 2.3. West-Mediterranean site and sampling set-up

In the West-Mediterranean basin, a 0.5-km long T-sensor mooring was deployed about 40 km south of Toulon-harbor, France. The relevant mooring information is given in Fig. 1a and Table 1. The area is known for strong boundary current flow instabilities and associated meandering with (sub-)mesoscale eddy-formation (Crépon et al., 1982; Albérola et al., 1995; Testor and Gascard, 2006) and occasional deep dense water formation due to late winter cooling and drying of relatively warm, salty East-Mediterranean waters (e.g., Millot, 1999). As a result, apparent density inversions are expected in vertical temperature profiles due to partial salinity-compensation in a complex of different water masses that may vary over roughly 1–10 km horizontal distances.

For reference of vertical temperature slope and to establish local temperature-density relationship, shipborne CTD-profiles were obtained to within 1 km from the mooring site during the deployment and recovery cruises, and 6 km to the northeast two years later. For the three profiles, three different CTD's were used, from different owning organizations. In November 2017 and October 2020 a SeaBird SBE911 CTD was used sampling at a rate of 24 Hz, with CT-sensors last calibrated in October 2017 and May 2020, respectively. In September 2018, a SeaBird SBE19 was used sampling at a rate of 1 Hz, with CT-sensors last calibrated in October 2017. The different robustness of the two types of CTD's is accounted for in the presentation of their data.

### 2.4. Challenger Deep site and sampling set-up

A 7-km long mooring was deployed in the Challenger Deep, Mariana Trench East-Pacific, close to the deepest point on Earth (van Haren, 2020). The relevant mooring information is given in Fig. 1b and Table 1. The 7-km mooring-length was born out of necessity as hadal-rated buoyancy was not available and current meter CMs and some T-sensors were rated to  $6 \times 10^7 \text{ N m}^{-2}$  only. Two sections of instrumentation were in the mooring. Only corrections to the deepest set of moored T-sensor data will be discussed for which data from one CM are required to describe surface tidal motions and mooring deflections. The other CM was intended for back-up and its data can be used to calculate vertical current shear (not considered here). The mooring was set-up for studies on internal waves, specifically with tidal frequency, and associated turbulence through their breaking with potential effects on nutrients and suspended matter transport in a deep, funnel-shaped ocean-trench.

Three shipborne 24-Hz sampled SeaBird 911 CTD-profiles were obtained at about 1 km from the mooring site. The CTD used in November 2016 had CT-sensors that were last calibrated in September 2015. The CTD used in November 2018 had CT-sensors that were last calibrated in October 2018.

**Table 1**

Mooring summary information. CM denotes single-point 2-MHz Nortek Aqua-Dopp current meter, which measures three components of water-flow velocity [u, v, w], pressure p and instrument tilt.

	West-Mediterranean Sea mooring	Challenger Deep mooring
latitude	42° 47.29'N	11° 19.59'N
longitude	06° 09.11'E	142° 11.25'E
seafloor-z	−2480 m	−10,910 m
deployment	18 November 2017 (yearday 321)	12 November 2016 (315)
recovery	15 September 2018 (257 + 365 = 622)	02 November 2019 (1035)
CM-z	−2310 m	−6100 m
CM-sampling	150 s	600 s
T-sensor-z	−2475 < z < −2372 m	−10,903 < z < −10,315 m
T-sampling	2 s	2 s
T->75% data	4.5 months	14 months

### 3. CTD-profile observations

Due to drift one year after calibration, CTD-temperature accuracy is no better than to within a range of  $\pm 0.0025^\circ \text{C}$  and CTD-salinity no better than  $\pm 0.003 \text{ g kg}^{-1}$ . These values are used in Figs. 2 and 3. It is seen that the deviations in near-bottom temperature and salinity values between two different profiles marginally exceed the ranges given above. The comparison of data with time is thus barely statistically significant in an absolute accuracy sense. The CTD-data are better used to infer relative values, i.e. to compare the vertical slopes in profiles of temperature, salinity and density anomaly between the different years.

#### 3.1. West-Mediterranean data

During the mooring deployment cruise in November 2017, the CTD was lowered to within 5 m above the seafloor. During the recovery cruise in September 2018, the CTD was stopped at  $z = -2400 \text{ m}$  due to winch constraints. The deep West-Mediterranean temperature data show small variations with depth  $O(0.0001)^\circ \text{C}/100 \text{ m}$  (Fig. 2). Between the two profiles obtained 10 months apart in time, considerable variation is seen in Conservative Temperature (Fig. 2a) and Absolute Salinity (Fig. 2b) at  $z > -2000 \text{ m}$ . Modest changes in density anomaly of about  $0.002 \text{ kg m}^{-3}$  denser waters are observed in November 2017 compared to September 2018 (Fig. 2c). For  $z > -1500 \text{ m}$ , the stratification is sufficient to support freely propagating internal waves in a frequency ( $\sigma$ ) band  $f \leq \sigma \leq N$  (e.g., LeBlond and Mysak, 1978) of at least one order of magnitude wide as  $N > 10f$ .

In deep waters for  $z < -2180 \text{ m}$ , magnifications (Fig. 2d–f) demonstrate that salinity contributions generally dominate over temperature contributions to density variations. The horizontal and vertical changes in density-anomaly values between and within the profiles are approximately 80% attributable to salinity contributions. (For reference, the standard local temperature/salinity variations ratio of 1/4.5 in terms of contributions to density variations is used to scale the x-axis ranges of Fig. 2d and e.) Whilst the noise in salinity observations also seems to dominate that in density variations, we cannot directly verify the absolute accuracy of the CTD observations and hence cannot verify the drift of the conductivity sensors.

Between  $-2380 < z < -2180 \text{ m}$ , the vertical temperature slope shows different sign in the profiles from 2017 and 2018 (Fig. 2d), while the vertical slopes of salinity (Fig. 2e) and of density (Fig. 2f) maintain the same (negative) sign reflecting stable vertical density stratification. The salinity slope also maintains approximately the same value. For this vertical range, the temperature-density relationship thus shows ambiguous values between the profiles and, most importantly, ambiguous sign. As a consequence, temperature cannot be used as a tracer for density variations and the moored T-sensor data cannot be used as a quantitative measure for turbulence, as is commonly employed for such data (e.g., van Haren et al., 2013). It is noted that in the T-sensor range between  $-2480 < z < -2380 \text{ m}$ , in the near-homogeneous lower 100 m above the seafloor, no sign-change is observed in the temperature-density relationship but magnitudes varied considerably between the 2017 and 2018 profiles and were ill-defined. In 2020, another CTD-profile was obtained 6 km from the mooring location. In that profile temperature dominated over salinity in contributing to vertical density variations.

In the vertical range of the present moored T-sensors,  $N$  calculated from CTD-profiles varies between 0 and  $2f$  (Fig. 2f), with a general overall mean value of about  $N = 1f = 1.36 \text{ cpd}$  (short for cycles per day) and maxima of small-1-m-scale buoyancy frequency  $N_s$  up to about  $N_{s, \text{max}} = 4f$ . As a result, the general mean range for the inertio-gravity wave (IGW) band is  $[\sigma_{\text{min}}, \sigma_{\text{max}}] = [0.6f, 1.7N] = [0.8, 2.3] \text{ cpd}$ . IGW-limits are computed as  $[\sigma_{\text{min}}, \sigma_{\text{max}}] = 1/\sqrt{2} \cdot [(A-B)^{1/2}, (A+B)^{1/2}]$  where  $A = N^2 + f^2 + f_s^2$  and  $B = (A^2 - (2fN)^2)^{1/2}$ , which results in limits below  $f$  and above  $N$ , respectively (e.g., LeBlond and Mysak, 1978). Knowledge of the very weak stratification is thus important for studies on particular



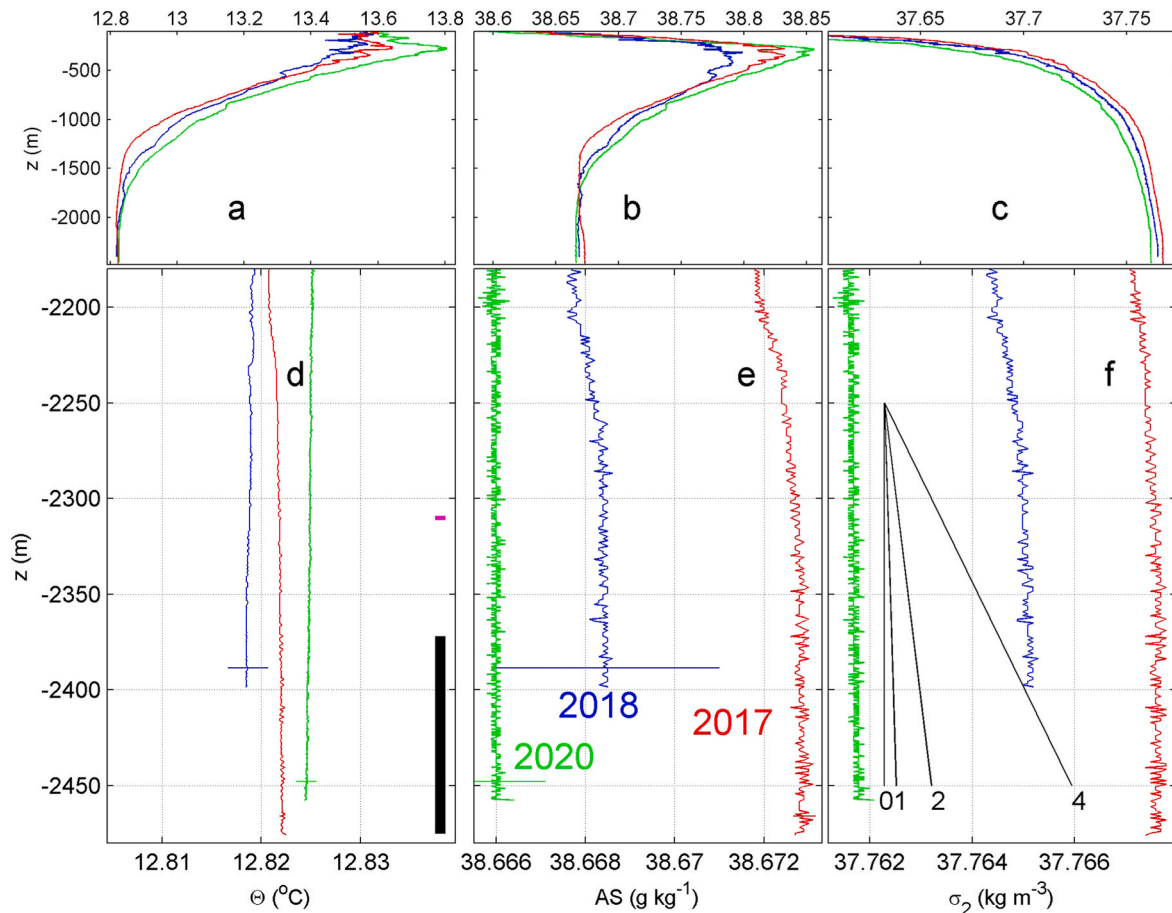


**Fig. 2.** Shipborne CTD-profiles obtained near T-sensor mooring site in the West-Mediterranean, in November 2017, September 2018 and, 6 km to the northeast, October 2020 (with lowest value 0.5 m above the local seafloor). In a.-c., vertical ranges are between the seafloor ( $z = -2480$  m) and  $z = -100$  m. In d.-f., magnifications are shown of  $-2480 < z < -2180$  m. The mooring site seafloor is at the  $z$ -level of the x-axes. (a,d) Conservative Temperature. In d., the vertical black bar indicates the vertical extent of the moored T-sensors. The purple dot indicates the location of the CM. The thin horizontal lines indicate the 'stability error' attributed to drift as inferred from [SeaBird \(2015, 2016\)](#) using the time after most recent calibration. The x-axis has the same range as in e., in terms of density contributions. (b,e) Absolute Salinity. (c,f) Density anomaly referenced to  $2 \times 10^7 \text{ N m}^{-2}$ . In f., four vertical slopes are drawn equivalent to those of buoyancy frequency  $N = 0, 1f, 2f, 4f$ , for reference.

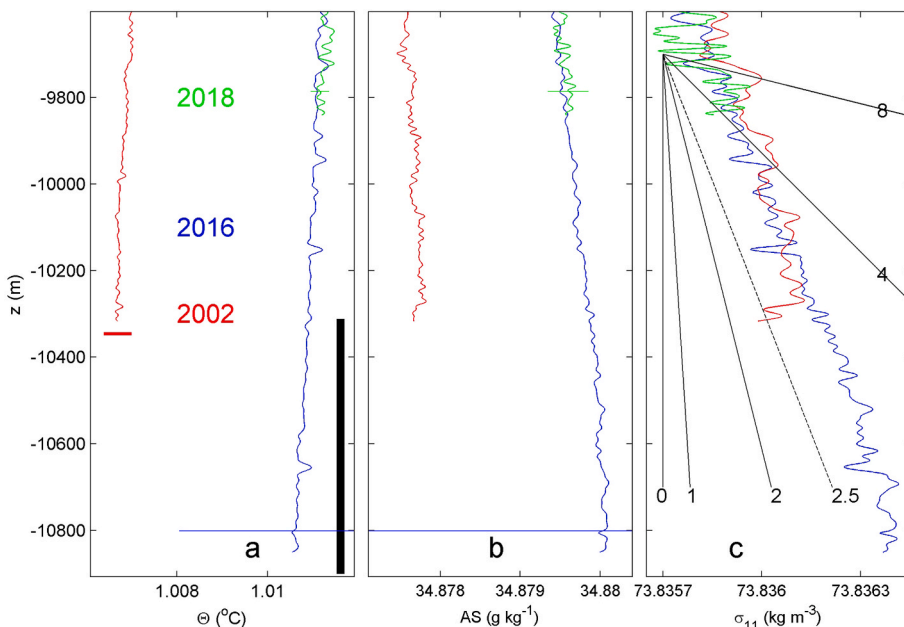


**Fig. 3.** As [Fig. 2d-f](#), but for magnifications of low-pass (noise-)filtered SBE911 CTD-profiles up to 1300 m above the seafloor near the deepest point from the Challenger Deep, Mariana Trench. The 2002 profile was from R/V Hakuho Maru where seafloor was at  $z = -10,346$  m (horizontal red line), the 2016 and 2018 profiles from R/V Sonne with seafloor at  $-10,907$  m ( $z$ -level of x-axes) but with different CTD-sensors each year. The 18 mm winch-cable on the Sonne was shortened by about 1.5 km in the years between the two profiles, so that the 2018 profile was stopped at  $-9850$  m while the 2016 profile at about  $-10,855$  m for safety reasons. The 2002 profile was stopped at about  $-10,315$  m locally. Various corrections and filtering of the data have been applied during the post-processing ([van Haren et al., 2017, 2021](#)). The 2018 salinity is deliberately off-set by  $-0.0034 \text{ g kg}^{-1}$  to fit in the frame of b. This value is equivalent to the (one-sided) bias or drift error value to the 2016 profile. Note that the temperature range in a. should be multiplied by a factor of 2.5 to compare with b. in terms of density contributions.

internal wave dynamics, which can only be achieved via careful post-processing applying necessary corrections to T-sensor data. Because of such stratification, the horizontal Coriolis parameter of the Earth rotational vector  $\Omega$  at latitude  $\varphi$  is  $f_h = 2\Omega\cos\varphi$  is no longer neglected (e.g., Saint-Guil, 1970). Its effects are zero for zonal propagation, because  $f_s = f_h\sin\alpha = 0$  for angle  $\alpha$  with respect to the zonal direction, but they are important for meridional IGW-propagation.

### 3.2. Challenger Deep data

The environmental conditions near the hadal deep seafloor of the Challenger Deep are approximately the same as in the deep West-Mediterranean but they are more stable in time. As the conditions of  $>10^8 \text{ Nm}^{-2}$  static pressure require shipborne CTD-profiling using specialized instrumentation and  $>12 \text{ km}$  long winch-cables, only a limited number of profiles can be compared from different years (Fig. 3). The static pressure conditions also impose elaborate post-processing with specific corrections of the CTD-data (van Haren et al., 2017,

2021). Over the 16 years of time-span, the profiles show a consistent pattern, of weak but persistent vertical stratification in density. It is noted that November-2016 data deviate by about the theoretical value for stability error or bias from November-2018 data.

Stratification provides mean  $N = 2-2.5f = 0.8-1.0 \text{ cpd}$ . Compared with the West-Mediterranean case, this value is more than doubling the value relative to local  $f$ , but about 0.7 times the absolute value. Both temperature and salinity consistently contribute to density variations albeit salinity still contributes most noting the exaggeration of the scale in Fig. 3a. The consistent contributions to density variations result in a tight temperature-density relationship, so that moored T-sensor data can be used to infer turbulence values. Relatively large small-scale stratification results in  $N_s = 8-10f$  in thin layers. The apparent inversions or unstable layers in CTD-profiles, best visible in temperature, are associated with episodic 100–200 m tall turbulent overturns or jets (van Haren, 2020; van Haren et al., 2021).

For drift-correction of moored T-sensor data the large-scale  $d\theta/dz$  from CTD-data in Fig. 3a are thus a consistent reference. The T-sensor

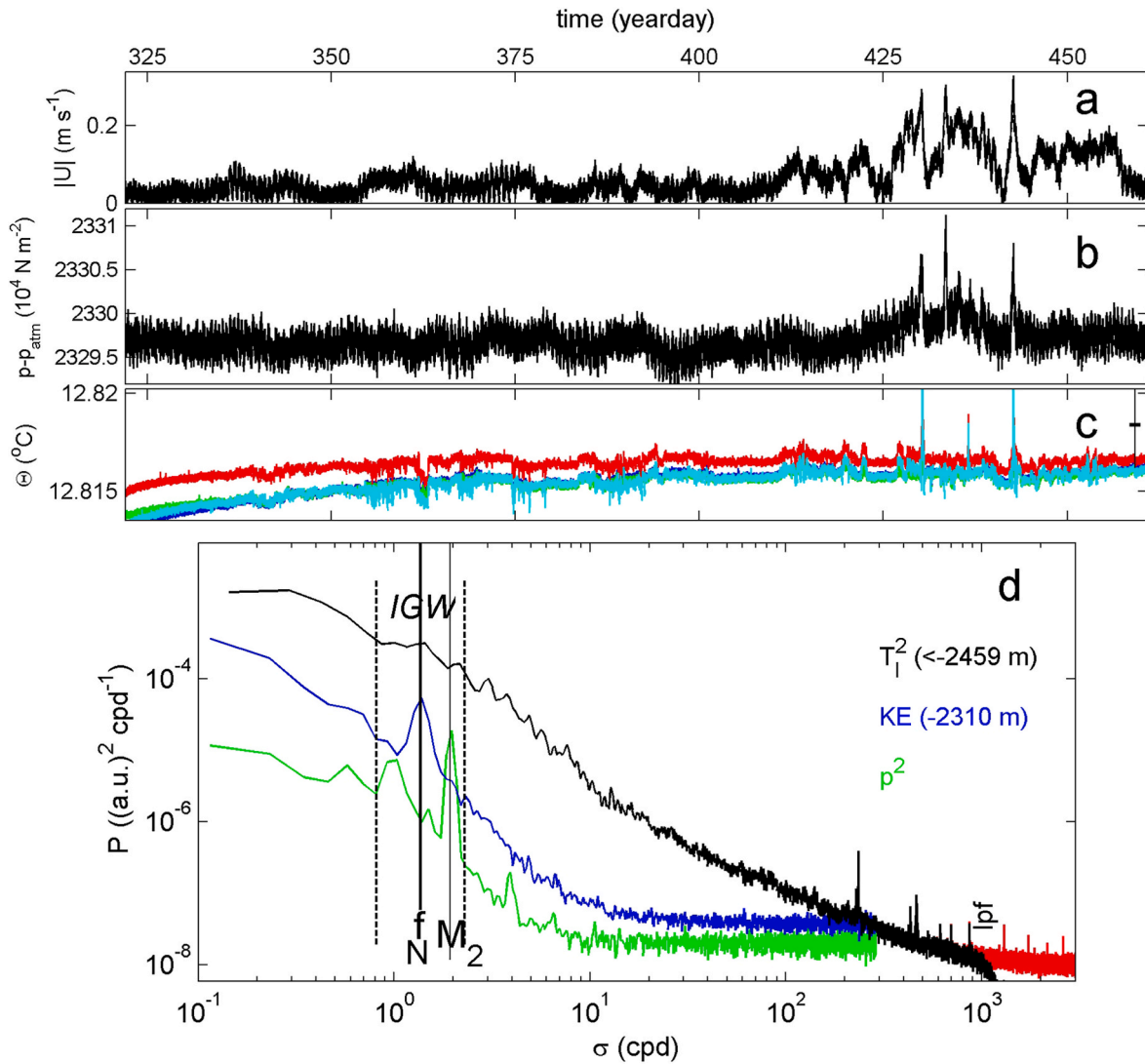


**Fig. 4.** Time series and spectra of 4.5 months of moored observations in the deep West-Mediterranean. (a) Horizontal water-flow amplitude observed by current meter (CM) at  $z = -2310 \text{ m}$ . (b) Sea pressure – atmospheric pressure observed at the CM. (c) Conservative Temperature from  $-2475 \text{ m}$  (blue),  $-2459 \text{ m}$  (green),  $-2393 \text{ m}$  (red) and  $-2377 \text{ m}$  (cyan). The data are compressibility-corrected with reference to CTD2018 on day 622 (mooring recovery), but not filtered and not drift-corrected. The black bar indicates the one-year drift error for CTD-data. (d) Power spectra for temperature variance, average for lower T-sensors at  $-2475 \text{ m}$  and  $-2459 \text{ m}$  (in red unfiltered; in black the low-pass filtered (lpf)-version cut-off at  $1000 \text{ cpd}$ ), in comparison with arbitrarily vertically shifted CM-data from  $-2310 \text{ m}$ : pressure ( $p$ ) variance and horizontal kinetic energy (KE). Inertial frequency  $f = N$  (buoyancy frequency) and semidiurnal tidal frequency  $M_2$  are indicated inside the inertio-gravity wave IGW band between dashed vertical lines (see text).

data also have to be corrected for (surface) tidal motions and for mooring deflections.

#### 4. Mooring results for the West-Mediterranean

##### 4.1. General observations

The taut and relatively short T-sensor mooring remained almost unaffected by the environmental variations, also when water-flow speeds were up to  $0.35 \text{ m s}^{-1}$  in late winter (Fig. 4a). Pressure at the CM showed variations of  $<10^4 \text{ N m}^{-2}$  in excess of tide-dominated surface level variations (Fig. 4b). This excess corresponds to  $<1 \text{ m}$  vertical variations at  $z = -2310 \text{ m}$  due to mooring deflections. A single 4.5-month T-sensor record varied by no more than  $4 \times 10^{-3}^\circ\text{C}$ , of which half was due to electronic drift causing a  $<0.03 \text{ cpd}$  low-frequency non-linear increase of temperature with time, especially during the first month (Fig. 4c). Except for the (positive) peaks around days 430, 435 and 440 in late winter, the entire environmental temperature range of variation is smaller than  $0.001^\circ\text{C}$ .

The spectral overview in Fig. 4d for the 4.5 months of good T-sensor data demonstrates diurnal and semidiurnal peaks in the pressure record reflecting the sea-level surface hydrostatic tides, while the kinetic energy of local horizontal water-flows  $[u, v]$  is dominated by inertial (about 17.5-h periodicity) and sub-inertial (about 10-day periodicity) motions. Tidal flows are very weak in the area. The 4.5-month mean near-seafloor temperature variance spectrum does not show spectral peaks, but a rather flat IGW-band around  $f$ . For studying the IGW and turbulence portions of the spectrum, it is noted that these spectra can be made without instrumental drift correction. This is because drift only affects the low-frequency sub-inertial  $<0.03 \text{ cpd}$  part of the spectrum at levels exceeding the instrumental noise level. In short daily time series observations it goes unnoticed, as a drift of  $0.001^\circ\text{C mo}^{-1}$  is equivalent to  $0.00003^\circ\text{C d}^{-1}$ . This daily variation in (temperature) value is smaller than the  $0.00005^\circ\text{C}$  noise level of the moored T-sensors (when measuring the Wien bridge oscillator over 120 ms per sampling interval.)

##### 4.2. Special drift- and pressure-corrections for moored T-sensor data from near-homogeneous waters

If a smoothed local CTD-profile is not available for reference for a particular 4–7 day averaging period and given the variable vertical temperature slopes in the area (Fig. 2d), the common method to correct T-sensors for drift in well-stratified waters does not work properly for the present deep West-Mediterranean data under near-homogeneous conditions in which the vertical temperature slope is 10–100 times smaller in magnitude than the adiabatic lapse rate of about  $-1.7 \times 10^{-8}^\circ\text{C N}^{-1}\text{m}^2$ . (It is noted that this lack of a consistent reference vertical temperature slope can only be established from repeated shipborne CTD-profiling near the moored T-sensors.)

Alternatively, for proper drift correction not resulting in unrealistic unstable conditions, we here use portions of data in which  $d\theta/dz = 0 < 0.00001^\circ\text{C}/100 \text{ m}$ , which is measurable to within instrumental noise level of NIOZ4 T-sensors over the entire range of observations as in homogeneous waters. Such homogeneous waters exist in the deep West-Mediterranean as established from previous extensive CTD-observations, especially in the central and southern parts of the basin (e.g., van Haren and Millot, 2006). A method to detect them is via the strong reduction in temperature variance, theoretically to zero, as is required for turbulent mixing down to the level of pure homogeneity so that the mixing efficiency becomes negligible. Homogeneous waters cannot be mixed anymore. In observational practice, one settles with the value going down to instrumental noise level and being void from environmental signals.

Waters that are homogeneous to the precision that can be measured also exist in the northern part of the West-Mediterranean, as follows

with reference to the lower 100 m of the CTD-profiles in Fig. 2. There however, they are rarer and possibly less persistent than in the central and southern parts of the basin due to the dynamics involved with the influence and vicinity of the continental slope near the T-sensor mooring. Nevertheless, during the 4.5-month of good data, a few periods with a minimum of 30 min duration were identified where environmental temperature variations over 100 m vertical extent were not significantly different than NIOZ4 noise limits. Around day 439.05 such a column was found, which lasted about 45 min (Fig. 5a). Averaged over this period, the standard deviation in the mean profile went down by a factor of 36 to  $0.0000017^\circ\text{C}$ , as expected for pure random white noise for 1300 samples. Another homogeneous column was found on day 373 (66 days previously). Near-homogeneous layers seldom last longer than 1 h in the area, as seen in the present data from Eulerian-fixed-in-space moored observations.

The special drift-correction thus consists of the following two steps.

First, the mean smooth pressure-(adiabatic lapse rate)-corrected zero-slope temperature ‘reference’ profile for each of these  $>30 \text{ min}$  periods replaces the mean drift-affected values for each T-sensor in that period. The zero-slope smooth profile is referenced to CTD-data, for absolute accuracy values. Between two zero-slope periods one could interpolate the remaining drift per T-sensor, but this results in corrections that are not better than about  $0.0001^\circ\text{C}$ .

Second, best-fit polynomials are computed of orders that depend on the standard deviation of the drift with respect to the noise level as measured from the (peak-to-peak drift) data in (Fig. 5b). As the drift is time-dependent, this implies to replace remaining drift for each T-sensor by a value from an:

- order-2 polynomial fit to the vertical mean profile when the data are from a period  $<1$  week from the time of the reference profile (day 439 or 373) and showing  $<0.0002^\circ\text{C}$  drift,
- order-1 polynomial fit to the vertical mean profile when the data are from a period  $>1$  week and  $<3$  weeks from the time of the reference profile and showing  $>0.0002^\circ\text{C}$  but  $<0.0006^\circ\text{C}$  drift,
- order-0 polynomial fit to the vertical mean profile when the data are from a period  $>3$  weeks from the time of the reference profile and showing  $>0.0006^\circ\text{C}$  drift.

The change in order of secondary correction polynomial fit is directly visible in drift-uncorrected mean profile data (Fig. 5b). If this correction of, for example, typically  $0.0009^\circ\text{C}$  single-sided (absolute value) peak drift in Fig. 5b for data from Fig. 5c, were not applied, the images in Fig. 5c and d would not show any dynamic processes as these would be buried in the remaining drift of the T-sensors.

The above secondary (special-drift) correction can also be explained using alternative formulation: For an aged T-sensor, a single-sample drift-correction holds for two days before new drift exceeds the instrumental noise level-criterion of  $0.00005^\circ\text{C}$ . When we use the criterion of establishing stratification to within error of a SeaBird 911 CTD over a 100 m vertical range so that  $N \approx f$  (van Haren and Millot, 2006), a single order of magnitude more relaxed slope of  $0.0005^\circ\text{C}/100 \text{ m}$  holds for about two weeks around the correction period. Knowledge of such criteria is necessary to be able to apply drift-correction to T-sensor data valid during periods of two weeks (or two days), also in general for periods outside that of Fig. 5a.

The results are adequate drift-corrected time-vertical observations, immediately surrounding the homogeneous column (Fig. 5a), a month earlier (Fig. 5c) and three days later (Fig. 5d). In all panels the entire colour range from dark-red to dark-blue corresponds to  $0.0007^\circ\text{C}$ . Like in the CTD-observations (Fig. 2d), the mean vertical profiles for different portions of moored T-sensor data show varying vertical temperature slopes, including sign-change (Fig. 5b). The area is dominated by apparent convective turbulent motions, often with warmer waters below relatively cool waters, also lasting (more than) half a day (Fig. 5d). The convection is either fed from above via homogeneous columns, or from



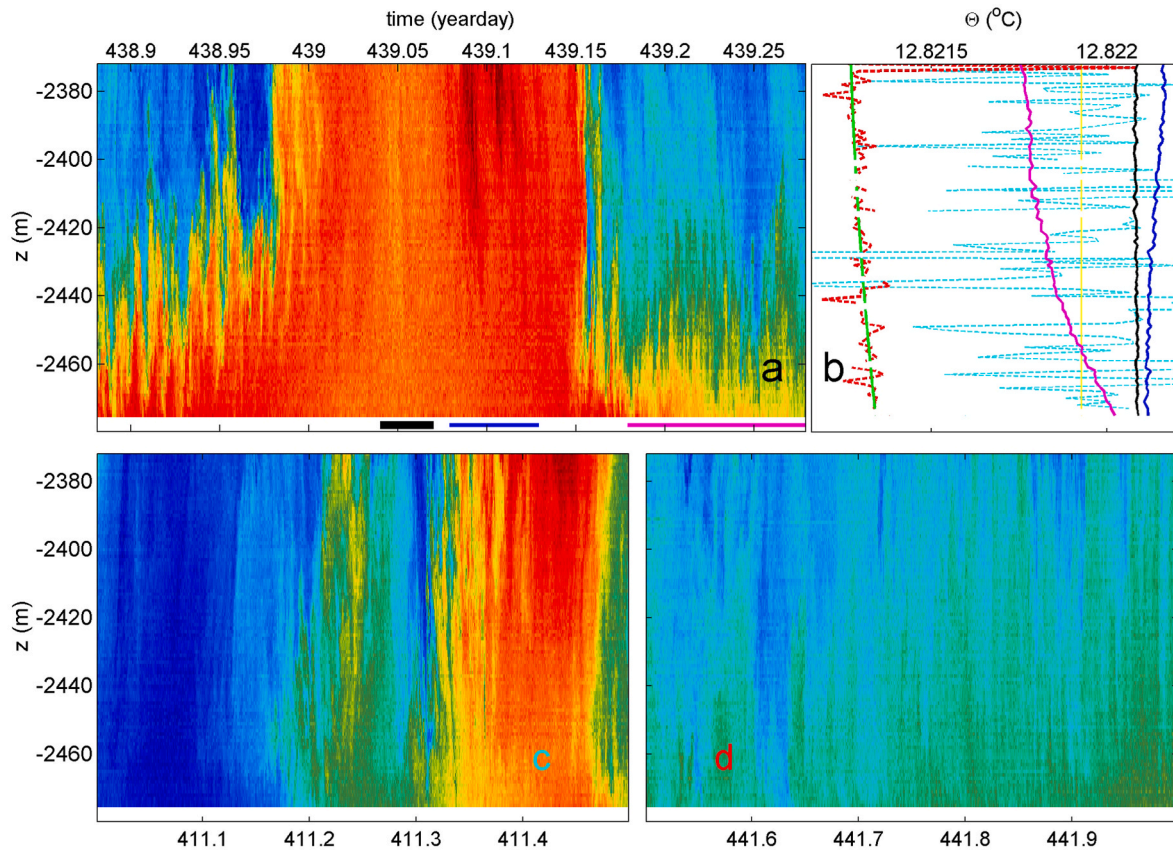


**Fig. 5.** Secondary drift- and pressure-correction of deep West-Mediterranean moored T-sensor data using a 103 m tall and 45 min duration homogeneous layer. (a) 9.6 h of low-pass filtered data removing instrumental white noise with cut-off at 1000 cpd (Fig. 4d), after applying laboratory calibration, drift-, and pressure-correction using the mean value for the period between days 439.04 and 439.07 (black horizontal bar) and referenced to local CTD2018 data. The entire temperature range from dark-red to dark-blue is  $\pm 0.00035$  °C around the mean value of the black bar. The seafloor is at the z-level of the time-axis. (b) Vertical profiles of mean values for periods indicated by black, blue and purple horizontal bars in a., in comparison with drift-dominated mean values of c. prior to secondary correction (light-blue, with order-0 best-fit in yellow) and d. (red, with order-2 polynomial best-fit in green). (c) Half day of data from 4 weeks prior to the data in a., after applying the order-0 best-fit to its mean value shown in b. for secondary drift-correction. The temperature range is the same as in a., but around a different mean value. (d) As c., but for data 2.5 days after those in a., after applying the order-2 best-fit to its mean value shown in b. for secondary drift-correction.

below via geothermal heating. In either case, the convection intensity is observed to vary with time, with typical temperature ranges of 0.0003 °C, for convection from below (Fig. 5a,d), and at least twice that amount, for convection from above (cf. also the positive peaks in Fig. 4c for extreme values).

Near-homogeneous waters do exist in layers larger than 100 m in the deep West-Mediterranean, see the CTD2017 profile for  $z < -2350$  m (Fig. 2f). In such a layer, salinity and temperature slopes may cancel each other in their density contributions. In a pure homogeneous case with density, salinity and temperature variations being homogenized, the maintenance of the adiabatic lapse rate requires active turbulence to avoid diffusive heat exchange with the surrounding environment. A homogeneous layer is thus not expected to consist of stagnant waters.

## 5. Mooring results for the Challenger Deep

### 5.1. General observations

The 7-km long mooring line in the Challenger Deep is in tidal flow waters (Fig. 6). While flow magnitudes measured at  $z = -6100$  m were modest,  $< 0.1$  m s<sup>-1</sup> (Fig. 6a), the long mooring line became regularly deflected by environmental water flows (Fig. 6b). In fact, 6-day periods of data under minimal mooring deflection of  $< 0.1$  m at  $z = -6100$  m are few and far between. This is likely due to the long mooring line with top-buoyancy extending about 2 km above the trench. Although not recorded, the current flow around  $-4000$  m where the top-buoys are located

is probably different from that within the trench.

Outside such periods, temperature time-series from  $z = -10,896$  m shows considerable tidal 14.5-day spring-neap cycle variations (Fig. 6c). However, the record from  $-10,326$  m additionally shows slow, about monthly, variations that mimic the pressure record at  $-6100$  m (Fig. 6b–d). The slow variations are thought to be induced by water flows induced by storms, as they cannot reflect ‘barotropic’ sealevel variations that would have been registered throughout the entire water column and also at the T-sensor at  $-10,896$  m.

In the area, the surface tidal amplitude is about 0.5 m. A surface vertical range difference between crest and trough of a wave of 1 m causes an adiabatic compressibility effect of about 0.0002 °C locally in the deep. When this is observed at all T-sensors, the result reflects an artificial internal tide with an excursion of several 100 m. This has to be corrected, under the notion that removing the tide will not affect eventual turbulence motions. Several special corrections are distinguished.

### 5.2. Special corrections for T-sensor data on a long mooring line in tidal flows and weakly stratified waters

To minimize and properly correct artificial effects during the post-processing of hadal Challenger Deep moored T-sensor data, it is easiest to find a period of about 6 days of negligible mooring deflections with  $\Delta z < 0.05$  m for the entire T-sensor range so that potential artificially induced temperature variations are  $< 0.00001$  °C. A period of 6



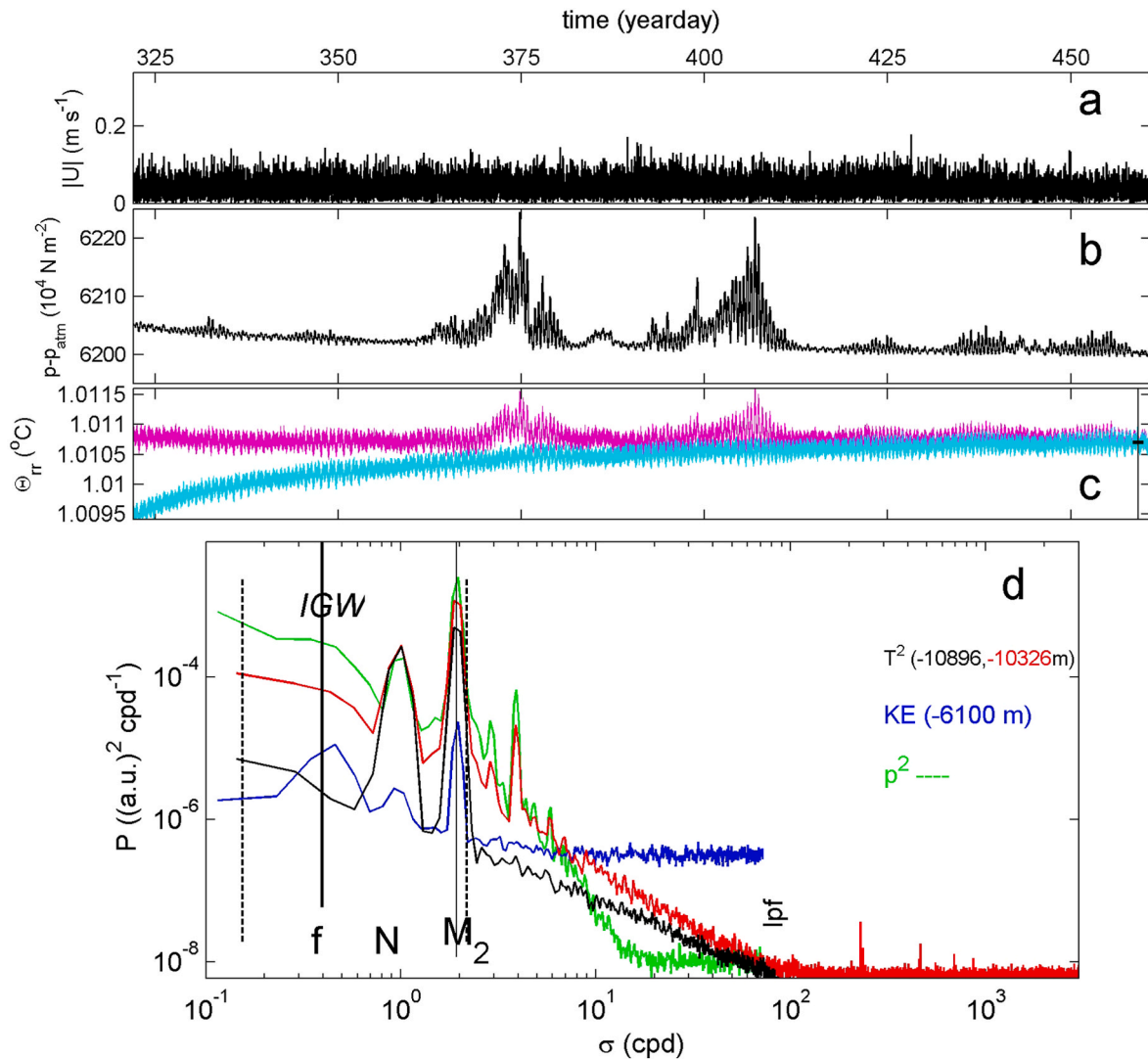


**Fig. 6.** As Fig. 4, but for Challenger Deep data, for a similar subset of timeseries. In a., the y-axis scale is kept the same. In b. and c. the vertical scales are different from those in Fig. 4. Recall that the CM is at about  $z = -6100$  m. In c., T-sensor data are from  $-10,896$  (light-blue) and  $-10,326$  m (purple). In d., the black and red temperature spectra are from  $-10,896$  m using  $\text{lpf} < 80$  cpd (black), and from  $-10,326$  m using no filter (red).

days is used as it exceeds the 2.5-day inertial period and because a 3-day change in drift value is smaller than two standard deviations of the instrumental noise level. Despite the generally large mooring deflections of the 7-km long mooring, at least two 6-day minimal mooring deflection periods are detected in pressure (Fig. 6b) (and tilt) records from  $z = -6100$  m.

The first special correction uses the observed information from the CM, foremost its pressure and tilt, to detect periods of minimal mooring deflection. Although the mooring line is not a stiff rod, the CM-information should in principle be portable to the  $z$ -level of T-sensors some 4.5 km below. However, as the easiest correctable static sealevel part is non-separable from the mooring deflection part especially in the tidal band, corrections can only be made when there is little or no mooring deflection. For such minimal deflection periods, an order-2 polynomial fit to the mean temperature profile is used and referenced to the smoothed CTD2016 temperature profile.

The second special correction covers the effects of large-scale surface waves, like tides, and mooring deflections of which a vertical displacement of  $\Delta z = 1$  m against the local adiabatic lapse rate of  $-1.93 \times 10^{-8} \text{ } ^\circ\text{C N}^{-1}\text{m}^{-2}$  shows as 200-m tall artificial internal waves that appear uniform without phase variation over the T-sensors' vertical range. Because the deep waters in the trench are almost homogeneous with  $d\Theta/dz = 5 \times 10^{-7} \text{ } ^\circ\text{C m}^{-1}$ , as is calculated from Fig. 3a and which is about 400 times smaller in value and opposite in sign compared to the local adiabatic lapse rate, mooring deflections create large artificial internal wave motions in the moored T-sensor data. This is remedied by transferring the fixed vertical position  $z$  for every T-sensor to functions varying with time,

$z_T(t) = z(2 - \cos(\text{ti}(t)))$

due to time-varying tilt  $\text{ti}(t)$  and computing the corresponding change in temperature as a consequence of the adiabatic lapse rate. The  $\text{ti}$  is the angle to the vertical of the vector composed of the CM's pitch and roll angles.

$$z_T(t) = z(2 - \cos(\text{ti}(t)))$$

Electronic filters are used to remove parts of the record that may contain artificial content. Harmonic analysis (Dronkers, 1964), using the functions by Pawlowicz et al. (2002), adequately removes the sealevel tidal variations, but does not remove some of the mooring deflections that may include (local) internal tidal motions. The harmonic analysis is applied to one of the lowest T-sensor records at  $z = -10,896$  m that shows minimal mooring deflections (Fig. 6c). The resulting harmonic series is then subtracted from all other T-sensor records. This is reasonably adequate, but again best during periods when the mooring does not move.

A third special correction also involves electronic filtering, but now using band-pass filters of portions of the data of some interest that are not affected by artificial signals and thus must lie outside tidal harmonic frequencies. This singles out most of the internal (tidal) wave band for detailed research and leaves the turbulence convective and inertial subranges available and easily accessible. For the present data, these subranges are found in the pass-band between [8, 80] cpd. Temperature variance at higher frequencies >80 cpd is dominated by (instrumental) white noise (Fig. 6d). Signals between 2 and 8 cpd may be used for study during some time periods and at some z-levels when not infected by higher tidal harmonics like  $M_4$  due to mooring deflections.

For all special corrections, the background stratification and absolute temperature reference value are inserted from the CTD-profiles in Fig. 3. This is the last of about 8 steps in post-processing of deep Challenger Deep T-sensor data. An example of the post-processing is given in four images in Fig. 7 for a period of relatively modest ( $\Delta z < 2.1$  m at  $z = -6100$  m;  $< 0.23$  m at  $-10,326$  m) mooring deflection. The raw data (Fig. 7a) do not show dynamical processes and reflect T-sensors with electronic problems but also misfits of about  $0.01$  °C (when values are transferred to SI units) that are recoverable after application of calibration and common drift correction (Fig. 7b). After compressibility correction, bad data interpolation, and mooring deflection correction, the surface tide is still visible with a trough-to-crest value artificially translated in isotherm displacements of about 150 m (Fig. 7c). The final corrected data (Fig. 7d), after subtracting harmonic analysis of T-sensor data at  $z = -10,896$  m and referencing to the mean vertical temperature slope of CTD-profile extrapolated to the seafloor, lack the regular

vertically uniform diurnal-modulated semidiurnal tidal excursions of Fig. 7c. Fig. 7d shows some internal tide (days 486–487,  $-10.8 < z < -10.5$  km), irregular turbulent overturning throughout the vertical range on day 488, and some sporadic warm temperature spurs in the interior, e.g. around day 487. The spurs are thought to have the same origin as instabilities visible in CTD-data (Fig. 3a).

The corrections of deep Challenger Deep T-sensor data are summarized in Figs. 8 and 9. For the longest time series of good data, pressure and tilt corrections are compared in terms of vertical excursions and their respective modifications to temperature at  $z = -10,326$  m (Fig. 8). The temperature data are reasonably corrected for mooring deflections, except during the largest excursions such as around day 760 (Fig. 8a). The harmonic analysis of the record from  $-10,896$  m to remove the surface tide generally works well for the record at  $-10,326$  m, and thus for all records in the T-sensor range, see a period with little mooring deflection around day 690, for example. During this period, the difference in tidal registration in pressure and tilt by the CM at  $-6100$  m is best visible (Fig. 8b). In terms of relative vertical variations  $dz$ , the pressure record  $dz_p$  shows the characteristic fortnightly spring-neap modulation of diurnal and semidiurnal surface tides, while the tilt record

$$dz_{ti} = h(1 - \cos(\pi t))$$

1

where  $h = 4800$  m denotes the distance to the seafloor, is nearly flat with negligible variation due to mooring deflection. As the local vertical surface tide barely exceeds 1 m, it is small in comparison with mooring deflections of up to  $dz = 50$  m at the CM. Hence, surface tides little affect

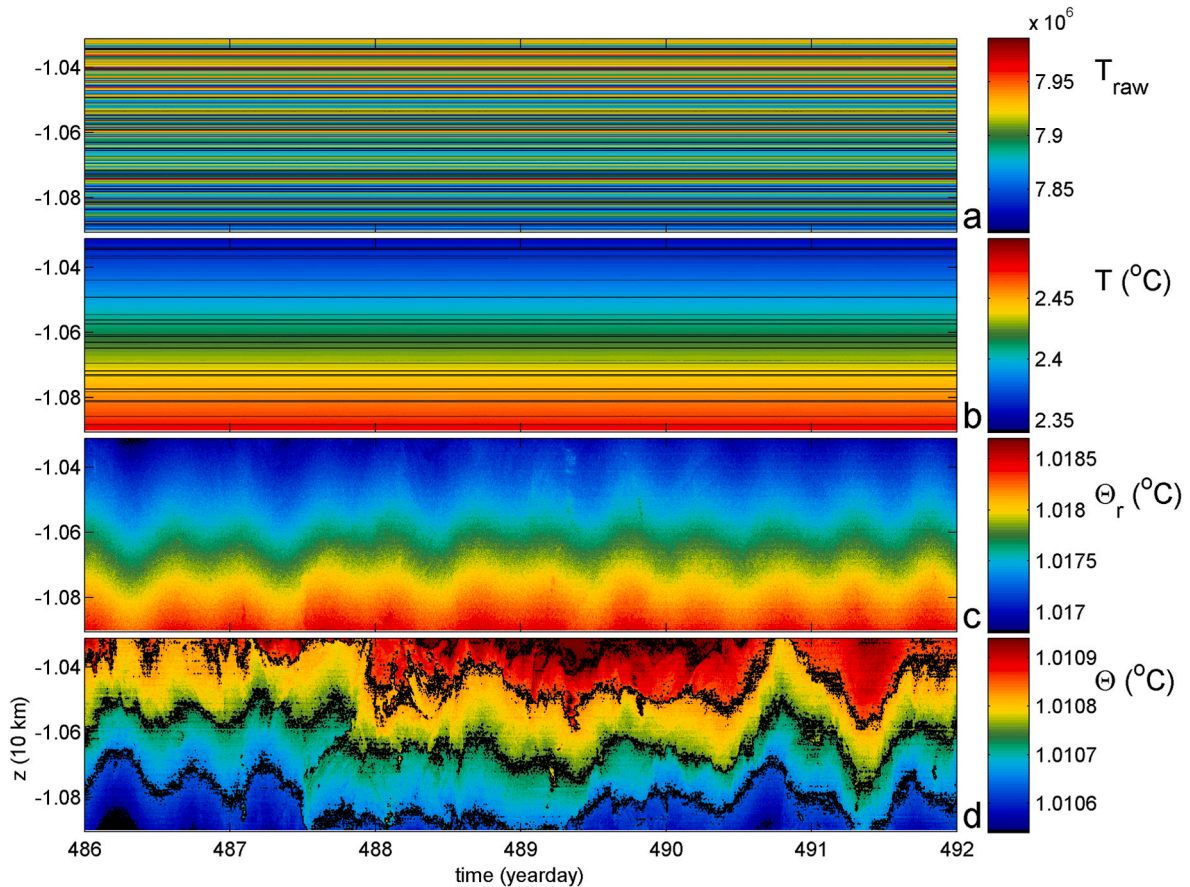


**Fig. 7.** Time-vertical plots of six days of Challenger Deep T-sensor data during moderate mooring deflections, displaying various post-processing steps. The local seafloor is at the z-level of the x-axis. (a) Raw data. (b) Data from a. but after transfer to SI units following calibration and following order-2 common smooth polynomial drift correction. The black horizontal lines indicate 'bad' T-sensor records due to calibration, battery or other electronic problems. (c) Data from b. but after bad-data interpolation, pressure-compressibility and first special correction. (d) Data from c. after final special correction and low-pass filtering with cut-off at 80 cpd (Fig. 6d). The black contours are drawn every  $0.0001$  °C, the entire colour range is  $0.0004$  °C.

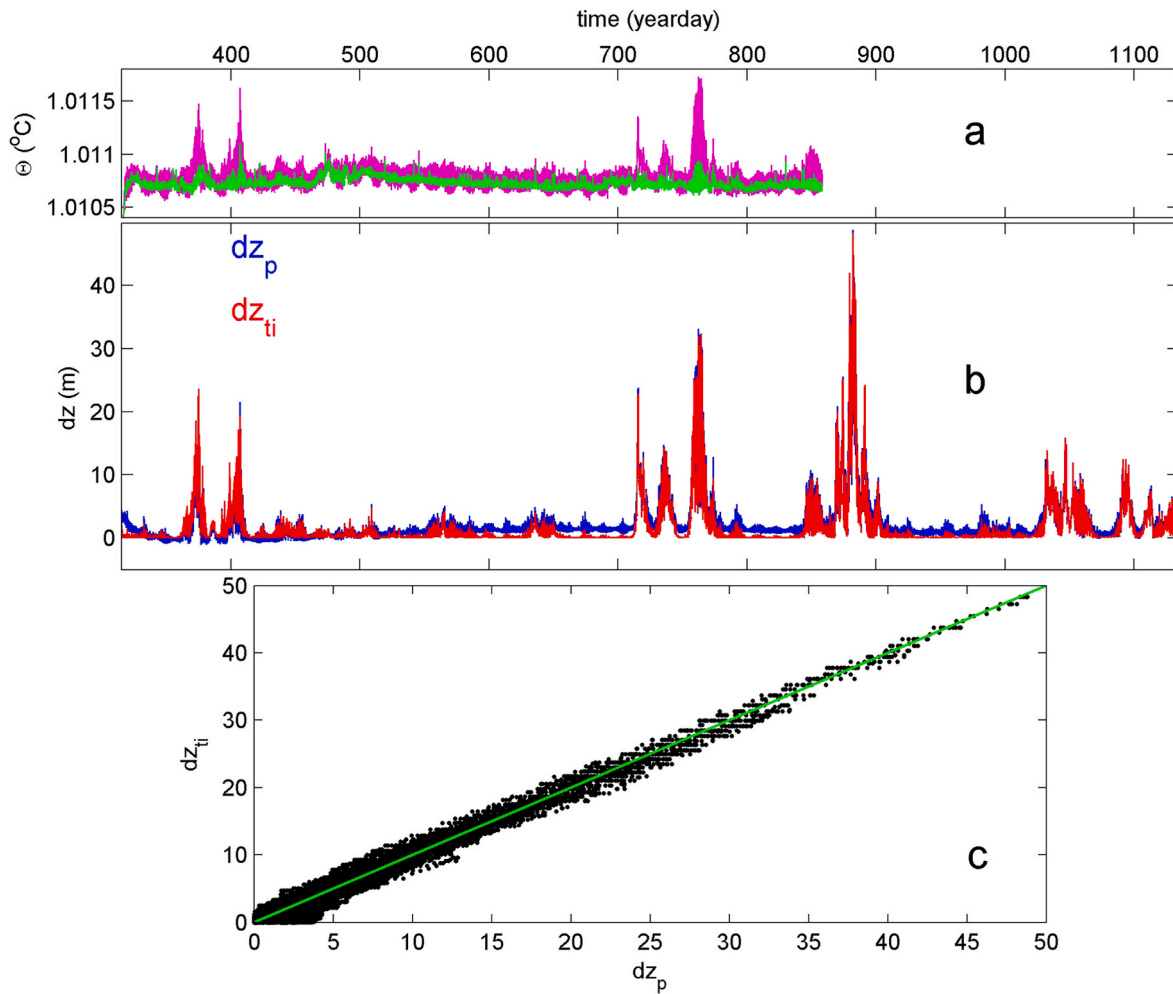


**Fig. 8.** Investigation using entire time series records of temperature correction due to mooring deflections calculated using tilt and pressure sensor information from the CM at  $-6100$  m. (a) 1.5-y Time series of Conservative Temperature at  $z = -10,326$  m before (purple) and after (green) correction for mooring deflection and surface tide. (b) 2.3-y Timeseries of pressure with values transferred to vertical variations (blue) and tilt-induced pendulum variations at  $-6100$  m following a best-fit tilt-factor of 1.105 (red). (c) Linear relationship between the two time series in b.

the nearly linear relationship between tilt and pressure registrations of vertical mooring deflections at  $-6100$  m (Fig. 8c).

Once corrected for moderate ( $dz < 2.1$  m at  $-6100$  m) mooring deflections, which result in relatively small ( $<0.23$  m) vertical deflections at  $-10,326$  m, and for harmonic analysis at  $-10,896$  m (Fig. 9a), the temperature records do not correlate with tidal motions that dominate mooring deflections (Fig. 9b). The corrections are thus adequate and the upper and lower temperature records show distinctive variations that are uncorrelated over the 570 m vertical scale and evidence genuine internal and turbulence motions at great ocean depths.

## 6. Discussion and conclusions

Although technically NTC-thermistors are robust and shock-resistant, the author found no evidence of tests performed on the stability or bias of CTD-temperature sensors upon a  $1 \text{ m s}^{-1}$  lowering through layers of different temperature. If a temperature-change effect exists on bias of CTD-sensors it will, together with the time-effect on bias, affect deep water mass characteristics that are based on high-resolution CTD-observations. It may be worth a future study.

As every NTC-thermistor has its own behavior, they are bought with tolerances within a certain limit and they are tested and tuned in the laboratory prior and after assembly with the main electronics. Nonetheless, their data require further corrections to obtain high-resolution

temperature information. The present corrections for deep moored T-sensor data were found to be  $< 0.001$  °C, and often  $O(0.0001)$  °C, but these are not small given their importance for the local internal wave-turbulence dynamics and variations therein. This puts a constraint on the instrumentation to be deployed in such waters, as well as on the corrections applied for mooring deflection and surface tide. Such corrections are already needed to achieve sufficient precision, or relative accuracy, as presented here.

The next challenge would be corrections to achieve absolute accuracy to within  $<0.0001$  °C. Such absolute-accuracy corrections other than CTD-referencing are not presented here, as they are not relevant for internal wave turbulence studies. For future moorings one requires instruments built with more stable electronics, if one wants persistent absolute accuracy of  $<0.0001$  °C.

The conclusions to achieve high-precision moored T-sensor data can be summarized as follows. The successful corrections for moored deep-sea T-sensor data must be employed with necessary information from additional sensors. In all cases, one needs nearby shipborne CTD-data to establish local temperature-density relationship and smoothed vertical temperature slope over the range of moored T-sensors. Preferably repeated CTD-profiles are used for verification of T-S relationship variability such as in Mediterranean waters and polar regions. It is recommended to calibrate the CTD-sensors as close as possible to the time of their use at sea, also when their data are used for water mass analyses.

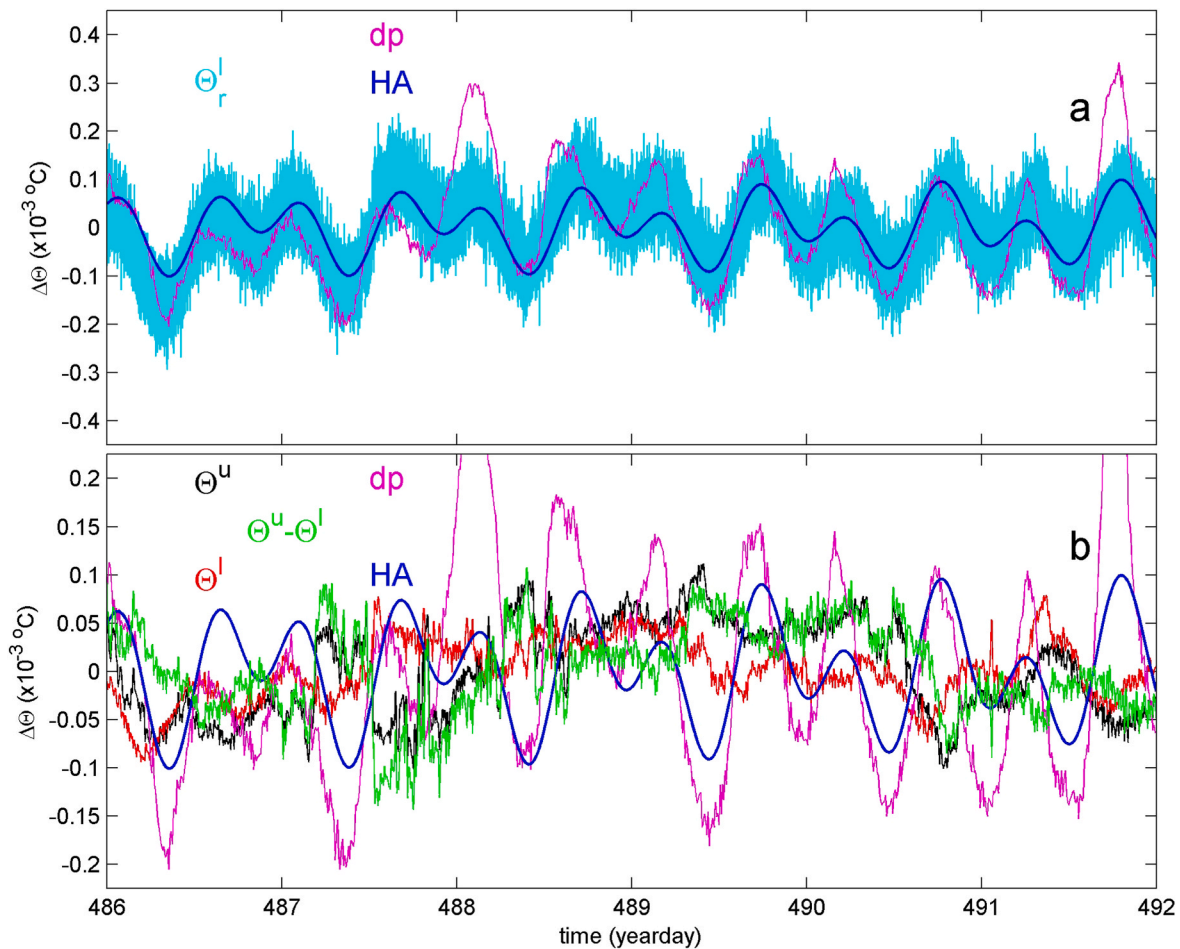


**Fig. 9.** Checks and balances of all corrections for data in Fig. 7. Pressure variations are transferred to temperature variations using the local adiabatic lapse rate of  $-1.93 \pm 0.03 \times 10^{-8} \text{ } ^\circ\text{C N}^{-1} \text{m}^{-2}$ . (a) The unfiltered temperature record at  $z = -10,896 \text{ m}$  (light-blue) with its harmonic analysis (blue) in comparison with the pressure compressibility record due to the surface tide (purple) during moderate mooring deflection of  $<2.1 \text{ m}$  at  $-6100 \text{ m}$ ,  $<0.23 \text{ m}$  at  $-10,326 \text{ m}$ ,  $<0.006 \text{ m}$  at  $-10,896 \text{ m}$ . (b) Low-pass filtered upper ( $-10,326 \text{ m}$ ; black) and lower ( $-10,896 \text{ m}$ ; red) temperature anomalies and their difference (green) in comparison with pressure sensor compressibility effects (purple) and harmonic analysis (blue) of a. Note the halved y-axis range.

For long moorings as deployed in the Challenger Deep, one needs moored tilt- and pressure-sensor information to correct for mooring deflections and surface displacements. Preferably such additional sensors are moored near the T-sensors. Mooring deflections are best minimized by making their lines as short as possible and by applying ample buoyancy. The study of unknown deep-sea dynamics is worthwhile with challenging high-quality instrumentation, which provide most satisfactory results in a custom-designed sub-surface mooring, albeit requiring careful handling and elaborate post-processing.

#### Declaration of competing interest

The authors declare the following financial interests/personal relationships which may be considered as potential competing interests:

#### Data availability

Data will be made available on request.

#### Acknowledgments

This research was supported in part by NWO, the Netherlands Organization for the advancement of science. I thank the captains and crews of the R/V I'Atalante, R/V Sonne and R/V Sally Ride, and NIOZ-MRF for their very helpful assistance during deployment and recovery of

the moorings. This paper benefitted from comments by anonymous reviewers.

#### References

- Alb  rola, C., Millot, C., Font, J., 1995. On the seasonal and mesoscale variabilities of the Northern Current during the PRIMO-0 experiment in the western Mediterranean Sea. *Oceanol. Acta* 18, 163–192.
- Cimatoribus, A.A., van Haren, H., Gostiaux, L., 2016. A procedure to compensate for the response drift of a large set of thermistors. *J. Atmos. Ocean. Technol.* 33 (7), 1495–1508.
- Cr  pon, M., Wald, L., Monget, J.M., 1982. Low-frequency waves in the ligurian sea during December 1977. *J. Geophys. Res.* 87, 595–600.
- Dronkers, J.J., 1964. *Tidal Computations in Rivers and Coastal Waters*. North Holland Publishing Company, Amsterdam, NL.
- IOC, SCOR, IAPSO, 2010. *The International Thermodynamic Equation of Seawater – 2010: Calculation and Use of Thermodynamic Properties*, Intergovernmental Oceanographic Commission, Manuals and Guides No. 56. UNESCO, Paris F.
- Kulkarni, A., Patrascu, M., van de Vijver, Y., van Wensveen, J., Pijnenburg, R., Nihtianov, S., 2015. Investigation of long-term drift of NTC temperature sensors with less than 1 mK uncertainty. *Proc. 24th IEEE Int. Symp. Industr. Electr.* 150–155.
- LeBlond, P.H., Mysak, L.A., 1978. *Waves in the Ocean*. Elsevier, Amsterdam, NL.
- Liu, M., Tanhua, T., 2021. Water masses in the Atlantic Ocean: characteristics and distributions. *Ocean Sci.* 17 (2), 463–486.
- Millot, C., 1999. Circulation in the western Mediterranean Sea. *J. Mar. Syst.* 20 (1–4), 423–442.
- Pawlowicz, R., Beardsley, B., Lentz, S., 2002. Classical tidal harmonic analysis including error estimates in MATLAB using T\_TIDE. *Comput. Geosci.* 28 (8), 929–937.
- Rhein, M., Stramma, L., Krahnemann, G., 1998. The spreading of Antarctic bottom water in the tropical Atlantic. *Deep Sea Res. Oceanogr. Res. Pap.* 45 (4–5), 507–527.
- Saint-Guilly, B., 1970. On internal waves. Effects of the horizontal component of the earth's rotation and of a uniform current. *Dtsch. Hydrogr. Z.* 23 (1), 16–23.



- SeaBird, 2015. SBE 9plus CTD, User Manual, p. 73.
- SeaBird, 2016. SBE 19plus SeaCAT Profiler CTD, User Manual, p. 101.
- Testor, P., Gascard, J.-C., 2006. Post-convection spreading phase in the northwestern Mediterranean Sea. *Deep Sea Res. Oceanogr. Res. Pap.* 53 (5), 869–893.
- van Haren, H., 2018. Philosophy and application of high-resolution temperature sensors for stratified waters. *Sensors* 18 (10), 3184. <https://doi.org/10.3390/s18103184>.
- van Haren, H., 2020. Challenger Deep internal wave turbulence events. *Deep Sea Res. Oceanogr. Res. Pap.* 165, 103400.
- van Haren, H., Millot, C., 2006. Determination of buoyancy frequency in weakly stable waters. *J. Geophys. Res.* 111 (C3), C03014 <https://doi.org/10.1029/2005JC003065>.
- van Haren, H., Morozov, E., Gostiaux, L., Tarakanov, R., 2013. Convective and shear-induced turbulence in the deep Kane Gap. *J. Geophys. Res. Oceans* 118 (11), 5924–5930. <https://doi.org/10.1002/2013JC009282>.
- van Haren, H., Berndt, C., Klaucke, I., 2017. Ocean mixing in deep-sea trenches: new insights from the Challenger Deep, Mariana Trench. *Deep Sea Res. Oceanogr. Res. Pap.* 129, 1–9.
- van Haren, H., Uchida, H., Yanagimoto, D., 2021. Further correcting pressure effects on SBE911 CTD-conductivity data from hadal depths. *J. Oceanogr.* 77 (1), 137–144.
- Wood, S.D., Mangum, B.W., Filliben, J.J., Tillett, S.B., 1978. An investigation of the stability of thermistors. *J. Res. Natl. Bur. Stand. (U.S.)* 83 (3), 247–263.